PROCEEDINGS OF THE INTERNATIONAL CONFERENCE NANOMATERIALS: APPLICATIONS AND PROPERTIES
Vol. **2** No 4, 04NEA05(4pp) (2013)

High-Quality Mega-Electron Volt Proton Beams Generated by Nanotube Accelerators

M. Murakami[1,*], M. Tanaka[2,†]

[1] *Institute of Laser Engineering, Osaka University, Suita, Osaka565-0871, Japan*
[2] *Department of Engineering, Chubu University, Aichi 487-8501, Japan*

(Received 20 May 2013; published online 31 August 2013)

Carbon nanotubes (CNTs) are hardy and versatile, with remarkable material and electronic properties. They could be also useful in some extreme conditions as well, when using a CNT as a shotgun barrel to shoot a beam of protons. The scheme nests two small hydrogen-rich fragments — which could be water ice, paraffin, or some other low-Z material — within a larger CNT that has gold atoms chemically adsorbed in its wall. The assembled structure is then zapped from the side with an ultraintense femtosecond laser pulse. The laser partially ionizes the gold and fully ionizes the hydrogen and carbon in the assemblage. After a few swings of the laser's electric field, significant numbers of electrons are blown off and form a cloud around the CNT. The now highly ionized coaxial structure generates a Coulomb potential in which the protons from the nanotube accelerator are squeezed toward the axis and accelerated out both ends of the CNT. The simulations indicate that even a non-optimized setup can produce highly collimated beams of nearly monoenergetic protons — 1.5 MeV for the parameters used. Such beams are of great interest in fields as diverse as medicine, fusion energy, and materials engineering.

Keywords: Ion Acceleration, Nanotubes, Proton Beams, CNT, MD Simulation.

PACS numbers: 41.75.Jv, 52.38.Kd, 61.46.Np

1. INTRODUCTION

In the past decade, ion acceleration driven by ultraintense femtsecond laser pulses has been intensively studied, because a number of future applications are expected, including cancer therapy [1], compact neutron sources [2], and ion-driven fast ignition [3] for medicine, industry, and fusion energy, respectively. For practical use of the accelerated ions, it is crucial to produce high-quality beams that are monoenergetic and collimated [4-6]. So far, work on the generation of quasimonoenergetic ions has been mainly based on a planar geometry. Other schemes with different geometries have been proposed using, for example, double-layer targets [7] or gas jet target [8]. Ramakrishna *et al.* [9] reported experimental evidence for quasimonoenergetic spectra of accelerated protons using water droplets. However, to produce high-quality ion beams is still in the process of research and development. An overall review on laser-driven ion acceleration has been recently published [10].

Carbon nanotubes (CNTs) [11] have extraordinary properties with respect to their material and mechanical properties. Usually CNTs are used as solid-state devices operating at relatively low temperatures and there have been no CNT applications at temperatures higher than 10^9 K and at time durations shorter than 10 fs. Here we propose an ion acceleration scheme with the use of CNTs, working at such an extreme circumstance. In the present concept dubbed a nanotube accelerator, a CNT, with fragments of low-Z materials embedded in it, is irradiated by an ultrashort intense laser to generate quasimonoenergetic collimated ion beams.

2. NANOTUBE ACCELERATOR

Figure 1 is a schematic of the nanotube accelerator. Inside the CNT, two smaller nanotubes are embedded. Typically the nanotube accelerator is irradiated by a 10 – 20 fs pulse having a laser intensity of between 10^{17} and 10^{19} W/cm^2. The outer carbon nanotube is chemically adsorbed with heavy atoms such as gold, while the inner nanotube is made of light materials such as hydrogen and carbon to form the bullets. Upon laser irradiation, electrons inside the nanotubes are ejected within a few laser cycles (comprising the small white particles around the nanotubes). The remaining nanotubes composed of positive ions generate a characteristic electrostatic Coulomb field so that the inner ions are accelerated along the axis symmetrically toward both ends of the outer nanotube. As a result, a pair of quasimonoenergetic collimated ion beams are obtained.

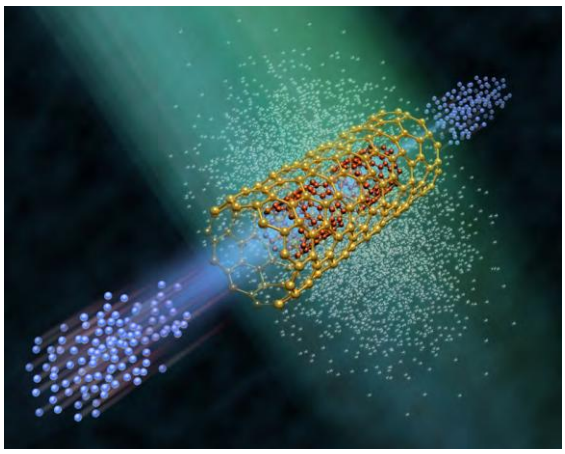

Fig. 1 – Schematic view of a nanotube accelerator

* Murakami-m@ile.osaka-u.ac.jp
† mtanaka@isc.chubu.ac.jp

This ultrashort pulse duration corresponds to the characteristic time of a Coulomb explosion [12-15] which is of the order of $2\pi/\omega_{pi}$ where ω_{pi} is the ion plasma frequency. Under such conditions, low-Z materials such as hydrogen and carbon are fully ionized, while materials such as gold are substantially ionized having $Z = 15$ - 25 at laser intensities [16] of 10^{18} W/cm^2. Significant numbers of electrons are then blown off by the intense laser field within a few laser cycles.

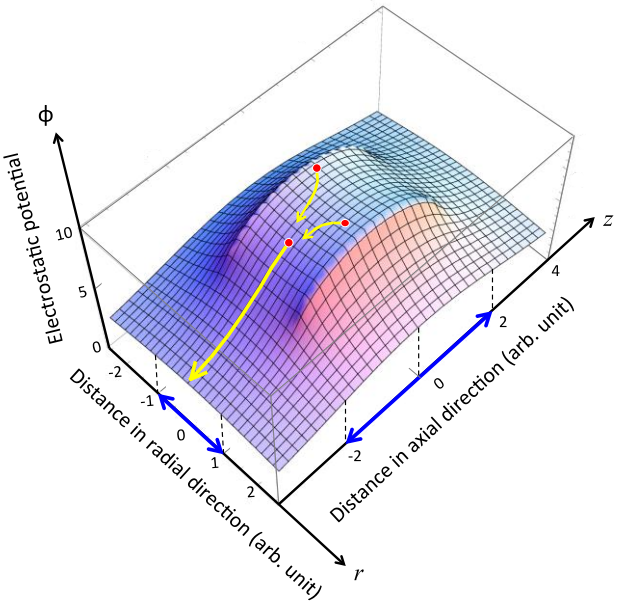

Fig. 2 – Characteristic Coulomb potential with a nanotube accelerator

3. SADDLE-SHAPED COULOMB POTENTIAL

Figure 2 shows a two-dimensional picture of the potential $\phi(r, z)$ obtained numerically. In Fig. 2, the influence of the inner low-Z nanotube upon ϕ is neglected because the total electric charge of the inner nanotube is much smaller than that of the outer nanotube. As a result of the saddle-shape potential, the interior ions get squeezed around the z-axis and accelerated along it, toward both ends of the CNT. Note that similar phenomenon to the squeezing effect has been reported, in which an injected diverging proton beam is bunched (squeezed) in a mm-long hollow cylindrical target [17]. Here we note, if electrons are distributed inside the cylinder, an electric field toward z-axis is generated, which is expected to enhance the squeezing effect.

In Fig. 2, some test ions (red dots) are also depicted schematically, how they are accelerated in the saddle-shaped potential field. The outer and inner nanotubes thus play the roles of the barrel and bullets of a gun, respectively. At positions around the CNT center, the potential gradients are relatively small along the z-axis. In other words, bullet ions initially located near the center will be accelerated quasimonoenergetically along the z-axis. It also turns out that the outer nanotube should not be too long, or $L/R \sim O(1)$, where L and R denote the axis length and the diameter of CNT, respectively. Otherwise the field inside the CNT is mostly null, leading to a degraded performance as an accelerator. Meanwhile, heavy atoms such as gold, that are chemically adsorbed on the carbon atoms of the CNT, reinforce the gun barrel and considerably enhance the acceleration performance of the bullet ions.

4. N-BODY SIMULATION

We have performed N-body charged particle simulations, in which all of the particle-to-particle Coulomb forces are computed exactly. The relativistic version of the Newtonian equations of motion are used, similar to molecular dynamics simulations of microwave heating of salty water and ice [18]. Moreover, our simulation includes the Lennard-Jones attractive potentials for pairs of like atoms, and repulsive potentials for other species as a core exclusion to avoid numerical divergences. Such N-body simulations are the most suitable numerical approach for treating parametric domains in which the plasma scale becomes significantly shorter than the Debye length. Note that recombination is not included in the present numerical model, which is justified under such a circumstance seen in the present scheme that stripped electrons are distantly blown off.

Figure 3 shows the temporal evolution of the dynamics of the nanotube accelerator, obtained from the N-body simulations. The CNT has an axial length of 30 nm and a diameter of 15 nm at which the gold atoms are chemically adsorbed to the carbon atoms. Inside the CNT, two cylindrical bullet nanotubes made of hydrogen are embedded, each of which has a diameter of 6 nm and an axial length of 6 nm. The initial distance between the two hydrogen bullets is 8 nm. Although hydrogen nanotubes do not actually exist in nature, that does not alter the physical mechanism of the nanotube accelerator, because the ionized bullets lose their original shape as they are squeezed toward the axis (see the time sequence of the top views in Fig. 3).

Here we give a few descriptions from an engineering point of view: The use of pure hydrogen clusters as the bullets is unpractical, because solid hydrogen atoms exist only at extremely low temperatures at around 250 degrees centigrade below zero. However, they can be easily replaced by such a hydrogen compound as water (H_2O) or paraffin (C_nH_{2n}), that can be solid at room temperatures. When such a compound is decomposed into fully ionized ions when irradiated by an intense laser, protons are to be selectively accelerated at higher quasi-monoenergetic speeds [15]. Pure carbon compounds like fullerenes or CNT are also tractable materials for the bullet. Insertion of nanometer-size structures into CNTs is another key issue. For example, producing CNTs containing fullerenes inside or multi-walled carbon nanotubes (MWCNT) has already been well established technically. Note that the size of the nanotube accelerator in Fig. 3 is the largest one that can be treated in our numerical environment using real lattice constants for the materials. The total number of charged particles for our simulations is about 4×10^5. At $t = 0$, sinusoidal laser light is incident on the nanotube from a radial direction perpendicular to the axis. The linearly polarized electric field is $E_L = E_0 \sin(2\pi T)$ for $T > 0$, where $T = t/t_0$ is the time normalized to the laser period $t_0 = 2.7$ fs for a titanium-sapphire laser at a wavelength of $\lambda_L = 0.8$ μm. In Fig. 3, the field amplitude is $E_0 = 3\times10^{12}$ V/m, corresponding to a laser intensity of $I_L = 10^{18}$ W/cm^2. At such an intensity, the gold atoms are photoionized to a state

of about Z_{Au} = 20 [16] while the carbon and hydrogen atoms are fully ionized to Z_C = 6 and Z_H = 1, respectively. Note that, in the present simulation, the averaged number of electrons that are effectively blown off from the nanotube is observed to be Z_{eff} = 17 - 18 per single gold ion. The maximum ion energy is expected to increase with the system size and laser intensity according to the principles of a Coulomb explosion [15].

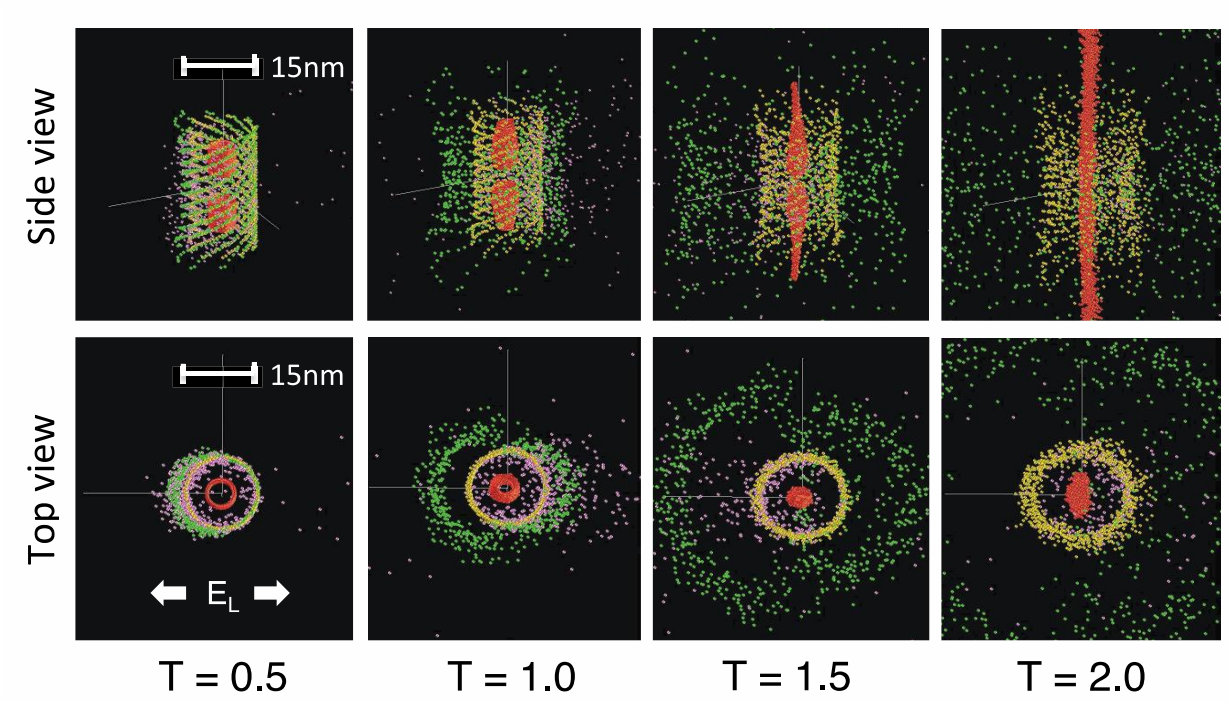

Fig. 3 – Snapshots of the nanotube accelerator dynamics at sequential times

In Fig. 3, the four snapshots correspond to the duration of the first two laser cycles (T < 2) at a constant increment of ΔT = 0.5. During the first cycle, many electrons are ejected by the intense laser field, which are already driven far away at the snapshot times and cannot be seen in Fig. 3. Simultaneously, the saddle-shaped Coulomb field of Fig. 2 forms to squeeze and accelerate the bullet ions along the z-axis. Quantitative performance is plotted in Fig. 4, where the spectrum of the kinetic energy component along the z-direction, ε_z, is seen to form a sharp quasimonoenergetic profile at normalized times of between T = 4 and 5. With the parameters that can be managed in our numerical environment, the energy is limited to ε_{max} = 1.5 MeV. The acceleration distance is roughly the half of the outer nanotube ~15 nm, that corresponds to an electrostatic force of the order of 10^{14} V/m, which is much higher than, for instance, a typical value expected in laser-plasma wake-field acceleration [19]. As long as monolayered nanotubes (in two dimensions) are used, the achievable ion energy ε_{max} is expected to increase linearly with the nanotube size L. If the nanotubes have a finite thickness (i.e., are three-dimensional), then one obtains another scaling law, $\varepsilon_{max} \propto L^2$. Furthermore, if the hydrogen atoms are replaced by carbon atoms, the kinetic energy of each carbon ion increases to about 10 MeV (the kinetic energy per nuclei is a bit smaller than in the proton case) for the same target structure as in Fig. 3, because the kinetic energy results from the initial potential energy which in turn is proportional to the electric charge. Note that for more practical simulations one needs to take account of a realistic laser pulse shape with a smooth envelope. As a matter of fact, we have verified that a quantitatively similar result to Fig. 3 in view of the energy spectrum is obtained using a Gaussian pulse with a full width at half maximum (FWHM) of five laser cycles under the same peak intensity. Retardation and magnetic effects in the electron-electron interactions will become crucial in the highly relativistic regime. However, working laser intensities for the present scheme are expected to be I_L = 10^{18} W/cm^2, and the relativistic effects mentioned above are not crucial.

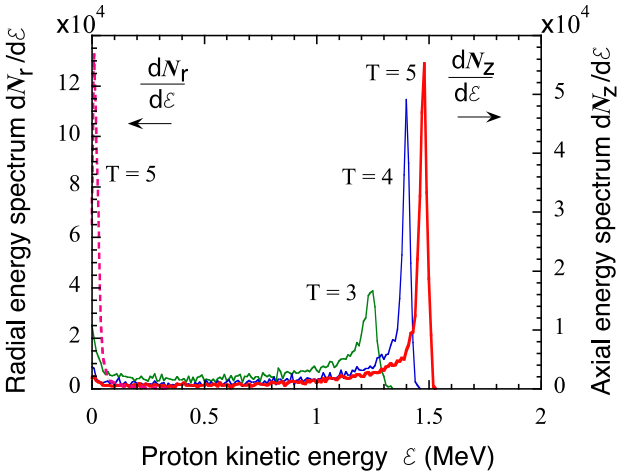

Fig. 4 – Temporal evolution of the proton energy spectrum in the axial (solid curves) and radial (dashed curve at T = 5) directions. The corresponding dynamics is shown in Fig. 3.

5. QUALITY OF THE PROTON BEAM

A good measure of the collimation is the energy ratio between the axis and the radius. As was seen in Fig. 3, the bullet ions are accelerated with a good collimation along z-axis. This longitudinal kinetic energy is approximately equal to the initial Coulomb energy, i.e., $\varepsilon_z \sim q(Q/X)_{\rm out}$, where Q and X are the total electric charge and a characteristic length of the outer nanotube in the early stage of the Coulomb explosion, respectively; q is the electric charge of the bullet ion. The scale length X can be approximately given by $X \sim \min(R, L)$. Meanwhile, the lateral (radial) kinetic energy of the bullet ions is brought about mainly by their own Coulomb repulsion, i.e., $\varepsilon_r \sim q(Q/X)_{\rm in}$, where $(Q/X)_{\rm in}$, is defined quite in a similar manner to $(Q/X)_{\rm out}$ but for the inner nanotube. Thus the energy ratio is estimated by $\varepsilon_z/\varepsilon_r = (Q/X)_{\rm out}/(Q/X)_{\rm in}$. In the case of Fig. 4, $\varepsilon_z \sim 1.5$ MeV and $\varepsilon_r \sim 0.017$ MeV in the final stage of acceleration, so that $\varepsilon_z/\varepsilon_r \sim 85$, which is rather close to a rough estimate obtained from the $\varepsilon_z/\varepsilon_r \sim 100$. These values of $\varepsilon_z/\varepsilon_r$ indicate a remarkably high degree of collimation. If the accelerated protons are kept ionized in flight without recombination, they are subject to long-range Coulomb forces. It might then be conjectured that the collimation performance of the beams can be degraded even at later times. However, the size of the bullet materials at T = 5 - 10 is already much larger than the initial size. In this stage, most of the Coulomb energy has already been converted into the kinetic energy, and thus the collimation will not be substantially degraded at later times.

The energy coupling efficiency η_c is an important index of the ion beam generation from an engineering point of view. It is defined as the ratio of the integrated kinetic energy of the bullet ions to that of all the electrons and ions at $t \to \infty$. The latter balances with the absorbed laser energy. In practical cases, the absorption efficiency of the system depends on how many nanotubes are in the focal region as well as the microscopic nanotube structure. In the present work, where the system is not optimized yet, the values of η_c are of the order of 1% or less [20]. However, the energy coupling efficiency is expected to be substantially improved by optimizing the target and laser parameters.

6. CONCLUSION

We have proposed an ion acceleration scheme using structured nanotubes, that operate under irradiance of ultrashort ultraintense laser pulses, to produce high-quality ion beams. Detailed three-dimensional particle simulation has demonstrated the generation of quasi-monoenergetic highly-collimated 1.5-MeV proton beams. The present concept leads to a view of CNTs different from an existing one, that until now had only been considered to be solid-state devices. It has been demonstrated that spatial control in nano-scale fabrication is as effective as temporal control in femto-scale laser operation. For further practical studies of the present scheme, it will be crucial that multiple nanotubes are uniformly produced in size and uniformly arranged in direction.

AKNOWLEDGEMENTS

This work was supported by Japan Society for the Promotion of Science (JSPS). The authors thank Profs. R. Hatakeyama and T. Kaneko of Tohoku University for discussions about carbon nanotubes. Present simulations were performed using Hitachi SR16000 system of National Institute for Fusion Science (NIFS), Japan.

REFERENCES

1. S.S. Bulanov, A. Brantov, V.Yu. Bychenkov, V. Chvykov, G. Kalinchenko, T. Matsuoka, P. Rousseau, S. Reed, V. Yanovsky, D.W. Litzenberg, and A. Maksimchuk, *Med. Phys*. **35**, 1770 (2008).
2. T. Ditmire, J. Zweiback, V.P. Yanovsky, T.E. Cowan, G. Hays, K.B. Wharton, *Nature* **398**, 489 (1999).
3. M. Roth, T.E. Cowan, M.H. Key, S.P. Hatchett, C. Brown, W. Fountain, J. Johnson, D.M. Pennington, R.A. Snavely, S.C. Wilks, K. Yasuike, H. Ruhl, F. Pegoraro, S.V. Bulanov, E.M. Campbell, M.D. Perry, H. Powell, *Phys. Rev. Lett*. **86**, 436 (2001).
4. S.C. Wilks, A.B. Langdon, T.E. Cowan, M. Roth, S. Singh, S. Hatchett, M.H. Key, D. Pennington, A. MacKinnon, R.A. Snavely, *Phys. Plasmas* **8**, 542 (2001).
5. T.E. Cowan, J. Fuchs, H. Ruhl, A. Kemp, P. Audebert, et al, *Phys. Rev. Lett*. **92**, 204801 (2004).
6. B.M. Hegelich, B.J. Albright, J. Cobble, K. Flippo, S. Letzring, et al, *Nature* **441**, 439 (2006).
7. T. Esirkepov, M. Borghesi, S.V. Bulanov, G. Mourou, T. Tajima, *Phys. Rev. Lett*. **92**, 175003 (2004).
8. K. Krushelnick, E.L. Clark, Z. Najmudin, M. Salvati, M.I.K. Santala, et al, *Phys. Rev. Lett*. **83**, 737 (1999).
9. B. Ramakrishna, M. Murakami, M. Borghesi, L. Ehrentraut, P.V. Nickles, et al, *Phys. Plasmas* **17**, 083113 (2010).
10. H. Daido, M. Nishiuchi, and A.S. Pirozhkov, *Rep. Prog. Phys*. **75**, 056401 (2012).
11. S. Iijima, *Nature* **354**, 56 (1991).
12. K. Nishihara, H. Amitani, M. Murakami, S.V. Bulanov, T.Zh. Esirkepov, *Nucl. Instrum. Methods Phys. Res. A* **464**, 98 (2001).
13. V.N. Novikov, A.V. Brantov, V.Yu. Bychenkov, V.F. Kovalev, *Fiz. Plazmy* **31**, 203 (2005).
14. Y. Fukuda, A.Ya. Faenov, M. Tampo, T.A. Pikuz, T. Nakamura, et al, *Phys. Rev. Lett*. **103**, 165002 (2009).
15. M. Murakami, K. Mima, *Phys. Plasmas* **16**, 103108 (2009).
16. P. Mulser, D. Bauer, *High Power Laser-Matter Interaction* (Heidelberg Berlin: Springer: 2010).
17. T. Toncian, M. Borghesi, J. Fuchs, E. d'Humieres, P. Antici, et al, *Science* **312**, 410 (2006).
18. M. Tanaka, S. Sato, *J. Chem. Phys*. **126**, 034509 (2007).
19. T. Tajima, J.M. Dawson, *Phys. Rev. Lett*. **43**, 267 (1979).
20. M. Murakami, M. Tanaka, *Appl. Phys. Lett.* **102**, 163101 (2013)